Coupling to a phononic mode in $Bi_{2-x}Pb_xSr_2CaCu_2O_{8+\delta}$: Angle-resolved photoemission

Beate Ziegler, Beate Müller, Alica Krapf, Helmut Dwelk, Christoph Janowitz, and Recardo Manzke
Humboldt-Universität zu Berlin, Institut für Physik, Newtonstrasse 15, 12489 Berlin, Germany
(Received 8 January 2007; revised manuscript received 30 January 2008; published 29 February 2008)

The kink in the dispersion and the drop in the width observed by angle-resolved photoemission in the nodal direction of the Brillouin zone of $Bi_{2-x}Pb_xSr_2CaCu_2O_{8+\delta}$ [(Pb)Bi2212] has attracted broad interest. Surprisingly, optimally lead-doped (Pb)Bi2212 with $T_C > 89$ K and the shadow band have not been investigated so far, although the origin of the kink and the drop is still under strong debate. In this context a resonant magnetic-mode scenario and an electron-phonon coupling scenario have been discussed controversially. Here we analyze the relevant differences between both scenarios and conclude that the kink and the drop are caused by a coupling of the electronic system to a phononic mode at least in the nodal direction. It is found that besides the dispersion and the drop in the width, also the peak height as a previously employed criterion can be used to define the energy scale of the interaction, giving a previously unknown means for a precise and consistent determination of the kink energy.

DOI: 10.1103/PhysRevB.77.054520 PACS number(s): 74.72.−h, 79.60.−i

I. INTRODUCTION

An important, but still open question is the coupling mechanism which causes high-temperature superconductivity. To come closer to an answer concerning possible coupling scenarios it is important to find excitations which are due to an interaction of the electronic system with a collective mode and to search for its origin. If such a mode is strong enough and correlates with other superconducting properties, then it could also be responsible for the pairing in high-temperature superconductivity. Therefore it is necessary to compare a large number of different high-temperature superconductors with the aim of finding common properties in the electronic structure. Such a common property is the kink in the dispersion of the main CuO-derived band in the nodal direction of the Brillouin zone. This kink is due to the coupling of the electrons to a collective mode and appears especially in Bi cuprates with $n=1$, $n=2$, and $n=3$ CuO_2 planes per unit cell. The bilayer components $Bi_{2-x}Pb_xSr_2CaCu_2O_{8+\delta}$ [(Pb)Bi2212] and Bi2212 are the most frequently studied ones of the Bi cuprates. The added lead suppresses the otherwise appearing $(\sim 5\times 1)$ superstructure, making the electronic structure of (Pb)Bi2212 simpler than that of Bi2212. Optimally lead-doped (Pb)Bi2212 with $T_c > 89$ K has not been investigated so far concerning the kink in the nodal direction. Also the behavior of the shadow band regarding the kink has not been considered up to now. Here we present a study of the kink in the dispersion and the drop in the width in the nodal direction of optimally doped ($T_c=93$ K) and slightly overdoped ($T_c=83$ K and $T_c=85$ K) (Pb)Bi2212 samples by use of angle-resolved photoemission spectroscopy, where we not only consider the main, but also the shadow band. Additionally an optimally La-doped (Pb)Bi2201 sample ($T_c=40$ K) was used for reference.

II. EXPERIMENTAL DETAILS

The high-quality samples used were grown out of a nonstoichiometric melt and were characterized by energy dispersive x-ray (EDX), ac-susceptibility, Laue diffraction, and low-energy electron diffraction (LEED) analyses. The samples were investigated by use of angle-resolved photoemission spectroscopy at the Synchrotron Radiation Center in Madison-Wisconsin. The measurements were done under UHV conditions with a Scienta SES2002 analyzer. A highest angle resolution of 0.1° and energy resolution of $\Delta E = 12.5$ meV have been achieved. The polarization of the radiation was parallel to the entrance slit of the detector. All measurements were done along the nodal direction, which means that the polarization was parallel to ΓX (or ΓY).

The high-temperature superconductivity of the Bi cuprates is associated with the two-dimensional CuO_2 planes, from where the signal near E_F originates. The photoemission intensity for a quasi-two-dimensional system is given by

$$I(\vec{k},\omega) = I_0(\vec{k}) f(\omega) A(\vec{k},\omega). \tag{1}$$

Here $\vec{k}$ is the momentum parallel to the surface, ω is the energy of the initial state relative to the chemical potential, f is the Fermi function, I_0 is proportional to the dipole matrix element $|M_{fi}|^2$ due to Fermi's golden rule, and A is the one-particle spectral function. The experimental signal is a convolution of $I(\vec{k},\omega)$ with the energy resolution and a sum over the momentum window plus an additive (extrinsic) background coming from secondary electrons. The essential result in angle-resolved photoemission spectroscopy (ARPES) studies is the spectral function $A(\vec{k},\omega)$, which can be expressed by using the retarded Green's function $G(\vec{k},\omega)$:

$$A(\vec{k},\omega) = -\frac{1}{\pi}\mathrm{Im}\, G(\vec{k},\omega) = \frac{1}{\pi}\frac{|\Sigma''(\vec{k},\omega)|}{[\omega - \epsilon_k - \Sigma'(\vec{k},\omega)]^2 + [\Sigma''(\vec{k},\omega)]^2}, \tag{2}$$

with self-energy $\Sigma = \Sigma' + i\Sigma''$ and bare dispersion ϵ_k. Furthermore, as can be seen by the generic expression for the spectral function $A(\vec{k},\omega)$ in Eq. (2) the peak position in an energy distribution curve (EDC) is determined by $\Sigma'(\vec{k},\omega)$ as well as $\Sigma''(\vec{k},\omega)$ because both terms are strongly energy depen-

dent. On the other hand, if the self-energy Σ is independent of $\vec{k}$ normal to the Fermi surface (and the matrix elements are a slowly varying function of $\vec{k}$), then the corresponding momentum distribution curves (MDCs) are simple Lorentzians centered at[1]

$$k = k_F + \frac{[\omega - \Sigma'(\omega)]}{v_F^0}. \tag{3}$$

This is obtained by approximating $\epsilon_k \simeq v_F^0 |(\vec{k} - \vec{k}_F)|$ in Eq. (2). v_F^0 represents the bare Fermi velocity normal to the Fermi surface.[2]

The full width at half maximum (FWHM) of the photoemission peak in a momentum distribution curve reflects the mean free path $l^* = 1/\Delta k$ such that

$$\Delta k = \frac{|2\Sigma''(\vec{k}, \omega)|}{v_F^0}. \tag{4}$$

Kordyuk *et al.*[3,4] employ a self-consistent determination of the real and imaginary parts of the spectral function with the bare Fermi velocity as input. But from Eqs. (2)–(4) it follows that it is necessary to know v_F^0 or ϵ_k [$\epsilon_k \simeq v_F^0 |(\vec{k} - \vec{k}_F)|$ for $\vec{k}$ near $\vec{k}_F$ (Ref. 2)] to get Σ' and/or Σ'' from a fit of the photoemission spectrum. v_F^0 or ϵ_k cannot be obtained directly from a photoemission spectrum. Nevertheless, the general behavior of Σ' and Σ'' is reflected in the dispersion and the FWHM curves, as Eqs. (3) and (4) show.

Generally the photoemission spectra, which are analyzed here, were fitted as follows. First, the Fermi energy of a sample was determined by fitting a spectrum of a thin gold film evaporated on the sample. Then, for normalization each spectrum was divided by such a spectrum of the sample covered with the gold film. The spectra were integrated over a window of 4 meV at the energy axis and over a window of 0.28° at the angular axis. From a complete spectrum series the momentum distribution curves are derived as a function of energy. These curves were fitted with a Lorentzian as indicated by Eq. (2). From the Lorentzian the peak height at peak maximum, the $\vec{k}$ position of the peak maximum and the FWHM were taken for further consideration.

III. RESULTS

Figure 1 shows typical momentum distribution curves, recorded in the nodal direction at a temperature of 20 K using a photon energy of 22 eV. One can see the main band, which crosses the Fermi surface near $k = 0.45$ Å^{-1}, and the shadow band, which crosses the Fermi surface near $k = 0.6$ Å^{-1}.

Beside the kink in the dispersion of the main band also the behavior of the shadow band concerning the kink will be considered here. In a recent investigation of the dispersion of the main and shadow bands of optimally doped Bi2201, underdoped (Pb)Bi2212, and underdoped Bi2212, Koitzsch *et al.*[5] found that the dispersions of the main and shadow bands show a similar behavior. The same has been found for the FWHM regarding size and behavior. But this publication did not treat the kink explicitly.

Fitting the spectra of optimally doped (Pb)Bi2212 as described in the previous section the following results were

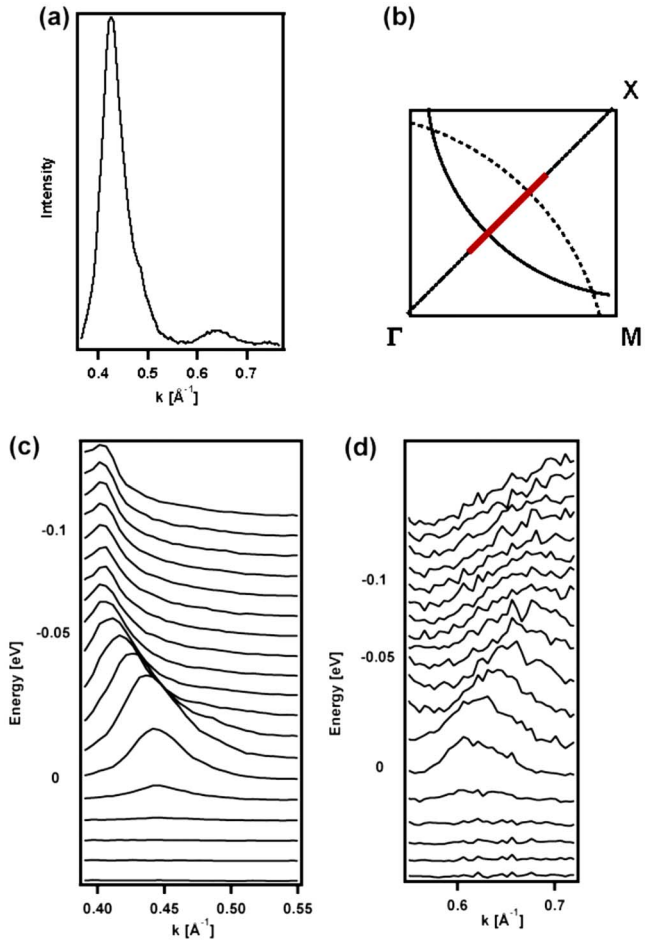

FIG. 1. (Color online) Momentum distribution curves (MDCs) of optimally doped (Pb)Bi2212 (sample 1) taken at 20 K with a photon energy of 22 eV. (a) MDC at 20 meV binding energy containing the main band and shadow band. (b) Measured direction of the Brillouin zone. (c) MDC's of main band and (d) shadow band.

obtained. Figure 2 shows the dispersion of the main (red squares) and the shadow band (blue circles). A kink near $\hbar\omega \simeq 60$ meV is clearly visible in the dispersion of both bands. In addition, both dispersions almost coincide, which is to be expected if the shadow band is of structural origin as Mans *et al.*[6] claim. Here we show that this is especially valid for the kink in the dispersion in the nodal direction.

Moreover, it can be observed that besides the kink in the dispersion, there is also a "kink in intensity" or more precisely a "kink in peak height." Additional to the commonly used criteria of dispersion and width, also the peak height shall be discussed as an additional and alternative means to define the energy position of the kink. Figure 3(a) shows a plot of the MDC peak height of the main band at the maximum of the peak as a function of $\hbar\omega = E - E_F$. One can clearly see a sharp kink near 60 meV, which corresponds to the position of the kink in the dispersion (see Fig. 2). Due to the restricted statistics, a less sharp kink in peak height is also visible in Fig. 3(b) for the shadow band.

The kink in peak height improves the ability to determine the precise position of the kink. Knowledge of the precise position of the kink is important to distinguish between the

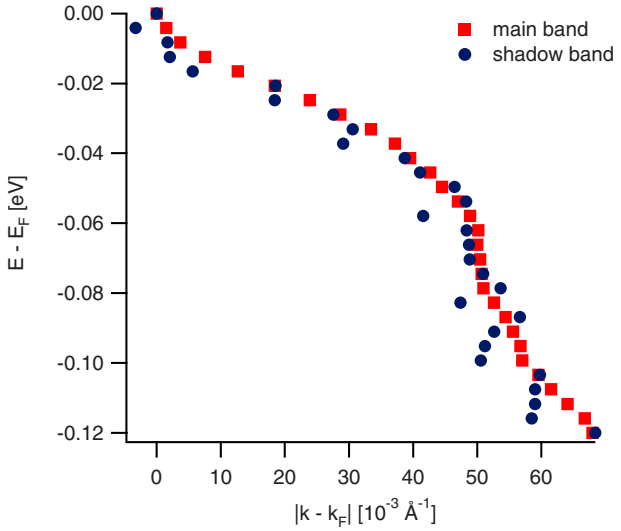

FIG. 2. (Color online) Dispersion of the main (red squares) and the shadow band (blue circles) of optimally doped (Pb)Bi2212 (sample 1).

different possible coupling modes, which are located at very similar energies (for details see Sec. IV). The kink in the peak height can qualitatively be understood in connection with a shift of spectral weight. Figure 4(a) shows the area under the momentum distribution curves as a function of $\hbar\omega = E - E_F$. For comparison the corresponding dispersion is plotted in Fig. 4(b). In agreement with theoretical calculations, which predict a splitting of the band into two branches at the energy of the coupling mode,[7] one can interpret the minimum between $\hbar\omega \simeq 30$ meV and $\hbar\omega \simeq 60$ meV in Fig. 4(a) as the region of low spectral intensity between the two split bands. This minimum and the kink in the peak height indicate that the spectral weight is shifted to lower binding energies and confirms the predicted two-branch behavior.

The interpretation of the FWHM curves, which are plotted in Figs. 5(a) and 5(b), is less straightforward. Around 60 meV, where the kink in the dispersion and the kink in peak height are situated, a drop occurs. The general line shape of the FWHM curve is consistent with published results of other (Pb)Bi2212 and Bi2212 samples (see, for example, Refs. 2, 3, and 8–10). But there is no general agreement about the determination of the position of the so-called "scattering rate kink" in the literature. Kordyuk *et al.*[3] usually take the onset of the drop as the kink position, but then the scattering rate kink in Ref. 3 is located around $\hbar\omega \simeq 100$ meV and not at the same position as the kink in the dispersion. Koitzsch *et al.*[10] did not discuss the position of the scattering rate kink. For nearly optimally doped (Pb)Bi2212 ($T_c = 89$ K) they found a kink in dispersion around $\hbar\omega \simeq 60$ meV and a drop in the scattering rate with an onset near $\hbar\omega \simeq 80$ meV and an offset near $\hbar\omega \simeq 40$ meV. Optimally doped (Pb)Bi2212 shows the same behavior [see Figs. 2 and 5(a)]. This result implies that the scattering rate kink is located at the half height between the onset and offset of the drop. The drop can be explained as an abrupt change of the mean free path $l^\star \sim 1/\Sigma''$ [see Eq. (4)] at the energy of the kink in the dispersion and the kink in the peak height.

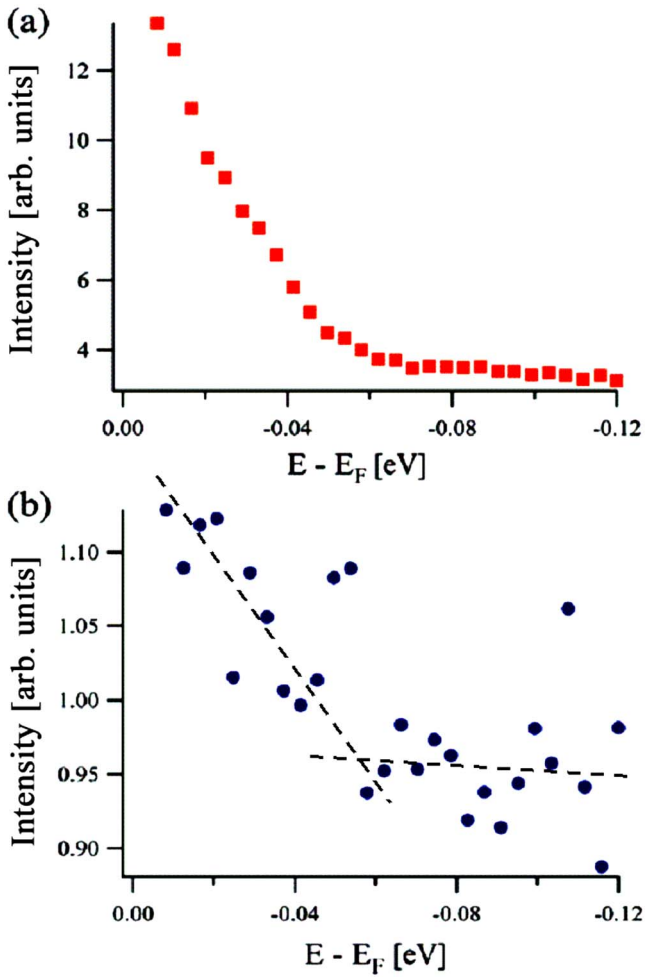

FIG. 3. (Color online) Intensity at peak maximum of the main band (a) and of the shadow band (b) of optimally doped (Pb)Bi2212 (sample 1). The black dashed lines are guides to the eye.

From a comparison of the FWHM curves in Figs. 5(a) and 5(b) with the corresponding dispersion and peak height curves (see Figs. 2 and 3), it can be concluded that the scattering rate kink is located at the half height between the onset and offset of the drop. So "drop" instead of "kink" charac-

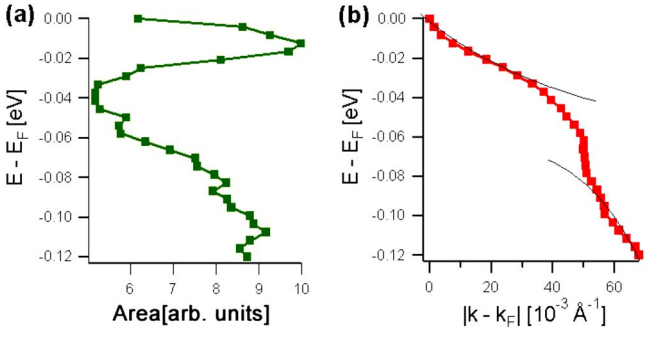

FIG. 4. (Color online) (a) Area under the momentum distribution curves of optimally doped (Pb)Bi2212 (sample 1) showing a minimum between $\hbar\omega \simeq 30$ meV and $\hbar\omega \simeq 60$ meV. (b) Dispersion of the main band of optimally doped (Pb)Bi2212 (sample 1). The black lines are guides to the eye.

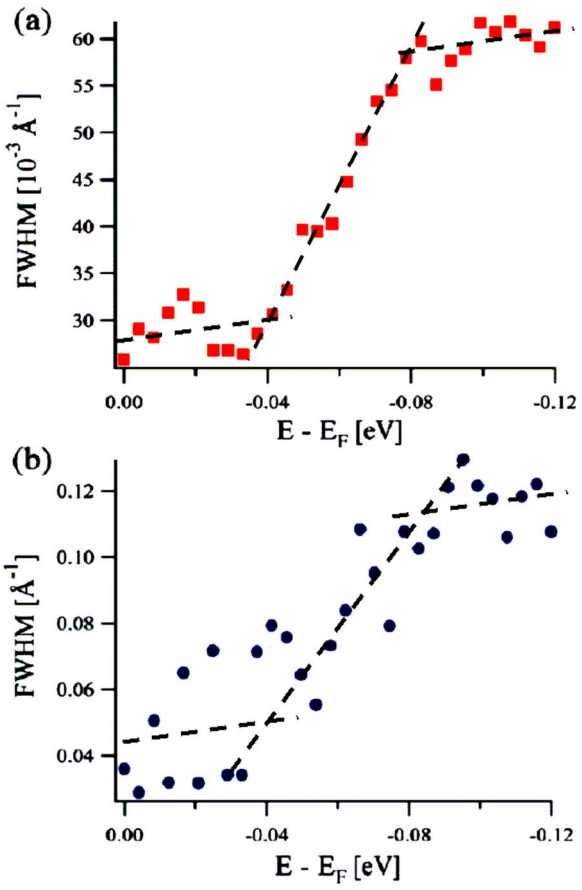

FIG. 5. (Color online) FWHM of optimally doped (Pb)Bi2212 (sample 1) of the main band (a) and of the shadow band (b). The black dashed lines are guides to the eye.

terizes more precisely the phenomenon observed here.

Also, the general line shapes of the FWHM curves of the main and shadow bands behave similarly, although a kink is hardly visible in Fig. 5(b) due to the restricted statistics. Although there are small deviations, the FWHM near E_F are the same in both bands, as also found in Refs. 5 and 6, but increase for higher binding energies.

Analogous results were obtained for the (Pb)Bi2201 sample, although the features appear less pronounced. This is shown in Fig. 6 where the kink in the dispersion, the kink in the peak height, and the drop in the FWHM of the main band appear near $\hbar\omega \simeq 60$ meV.

Table I shows the different samples studied, their transition temperature and Pb content, the number of analyzed spectrum series, and the obtained kink energy. No general trend for a scaling of the kink energy with T_c is observable. The averaged position of the kink, taking into account all analyzed spectra of (Pb)Bi2212 samples, is at $\hbar\omega_{\text{kink}} = (64 \pm 6)$ meV.

Measurements at different temperatures between 20 K and 120 K were performed at an slightly overdoped (Pb)Bi2212 sample ($T_c = 83$ K, sample 3) using a photon energy of 22 eV. In agreement with former published literature the kink in the dispersion persists at least up to $T = 120$ K and sharpens with decreasing temperature.[2,8] The drop in the width vanishes between 100 K and 120 K and is presumably related to

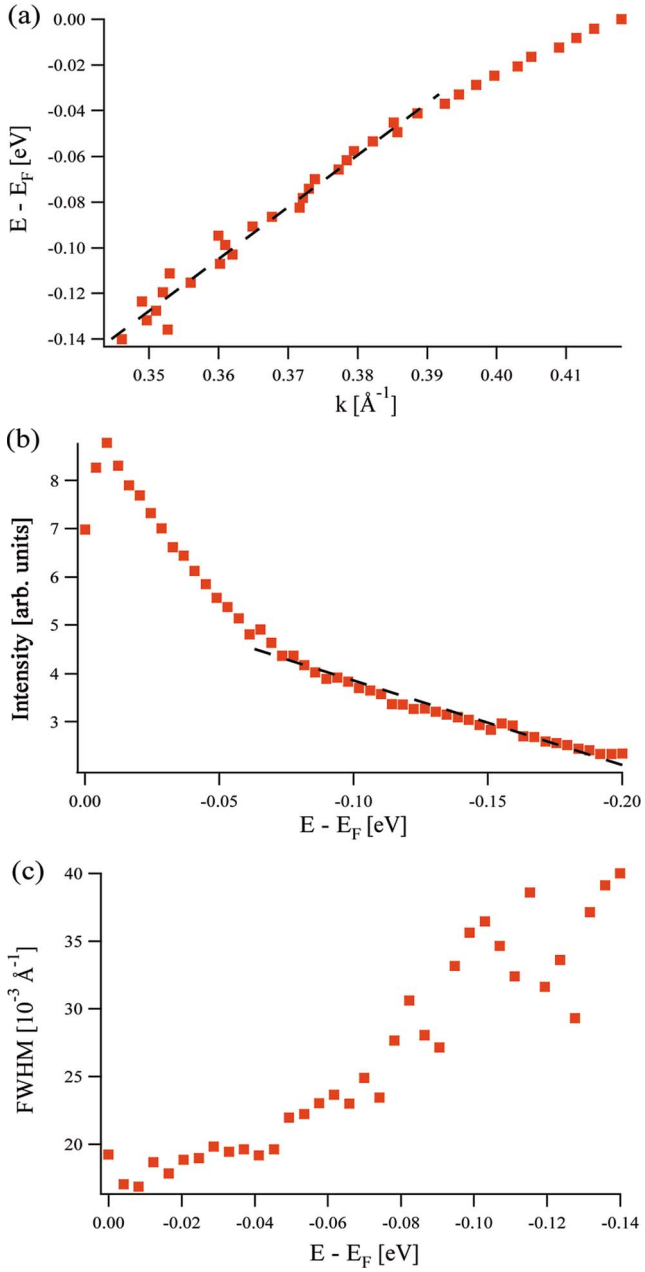

FIG. 6. (Color online) (a) Dispersion, (b) peak height, and (c) FWHM of the main band of optimally doped (Pb)Bi2201 (sample 4). Red squares: data. Black dashed line: guide to the eye.

the pseudogap temperature $T^\star$ and not T_c. In Fig. 7 the peak height at peak maximum is plotted for different temperatures. A closer look shows that the kink in the peak height around 65 meV gradually vanishes with increasing temperature and also disappears almost at 120 K. This indicates that the appearance of the kink is not connected with T_c, but presumably with $T^\star$.

IV. DISCUSSION

A coupling of the electronic system to a collective mode generally appears in photoemission data as a kink in the dispersion, a kink in the peak height, and a drop in the width.

TABLE I. The measured three different (Pb)Bi2212 samples 1–3 and (Pb)Bi2201 sample 4, their T_c, doping level, Pb content x, the number of analyzed spectrum series, and the kink energy $\hbar\omega_{\text{kink}}$.

Sample	T_c [K]	Doping	x	Number of spectrum series	$\hbar\omega_{\text{kink}}$ [meV]
1	93	opt. (O_2)	0.28	3	58 ± 6
2	85	overd. (O_2)	0.27	1	69 ± 5
3	83	overd. (O_2)	0.27	6	65 ± 5
4	40	opt. (La)	0.43	1	60 ± 8

If one compares these three features as criteria for a determination of the mode energy, then one has to realize that the kink in the peak height allows a very precise determination while the drop in the width is an unsure indicator (see especially Fig. 6). Together with the kink in the dispersion the kink in the peak height is a strong criterion for the determination of the energy where an interaction with a collective mode takes place. Since the angular scans only cover a very limited angular range, we expect the matrix element variations to be of minor importance for the peak height criterion.

Provided that the kink energy is a manifestation of the most prominent interaction of the electronic degrees of freedom with a boson, we concentrate on its discussion. At the present time two different coupling mechanisms are controversially discussed in the literature. The first one is based on the resonant magnetic-mode scenario and the second one on the electron-phonon coupling scenario. Two reasons complicate a decision between these two. First, the general manifestation of a coupling mode in ARPES spectra without further information does not allow one to decide between a phononic or a magnetic mode. In both cases the spectra would show a kink in the dispersion. Second, for Bi cuprates the magnetic and phononic modes are incompletely investigated.

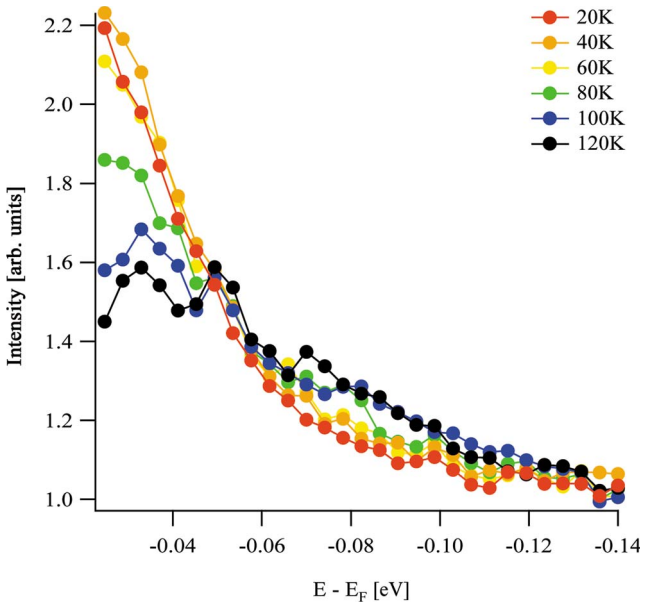

FIG. 7. (Color online) Intensity at peak maximum for different temperatures of slightly overdoped (Pb)Bi2212 (sample 3).

Magnetic resonance modes can generally be observed in inelastic neutron scattering (INS). But there are no published results of measurements on (Pb)Bi2212 and only a few on Bi2212 because the crystals typically grow as thin plates with a volume much too small for INS. The magnetic excitations in Bi2212 (Refs. 11 and 12) were observed at energies around $E_{\text{res}}=40$ meV scaling with T_c. A remnant of these modes persisted far into the pseudogap state. Further, a comparison of the results obtained from Bi2212 with those from $YBa_2Cu_3O_{6+x}$ shows that the energy of the magnetic resonance mode scales with T_c in both the underdoped and overdoped regimes.[12,13] Recently an additional magnetic mode was observed in $YBa_2Cu_3O_{6+x}$ at $E_{\text{res}}=57$ meV.[14]

Also phononic modes can be measured by INS. For the above-mentioned reasons there are no publications concerning (Pb)Bi2212 or Bi2212. But in $YBa_2Cu_3O_{6+x}$ phononic modes were observed at $E_{\text{res}}=55$ meV and $E_{\text{res}}=75$ meV independent of T_c.[15]

There are a lot of arguments in favor of both scenarios. So it is necessary to search for the differences between the two. First, it has to be realized that for both, the coupling to a photonic and to a bosonic mode, kinks in the photoemission spectra are expected at similar energies between 40 meV and 75 meV and persist presumably up to $T^{\star}$. The main difference is the observation that the energy of the magnetic resonance mode scales with T_c in contrast to the energy of the phononic modes. This means for ARPES measurements that the difference between magnetic and phononic coupling is the scaling of the kink energy with T_c in the magnetic case in contradiction to phononic coupling. The kink energies of the different samples are listed in Table I. For the three measured (Pb)Bi2212 samples no scaling of the kink energy with T_c is observed. Also former published measurements (see, for example, Refs. 8, 3, 10, and 16), covering a wide doping range did not show a dependence of the kink energy on T_c. This result argues against a coupling to the magnetic resonance mode. Furthermore it is consistent with results of photoemission measurements on $La_{2-x}Sr_xCuO_4$ (LSCO) in the nodal direction, where also no dependence of the kink energy on doping was found for a wide doping range.[17] Additionally the nodal kink in the dispersion is independent of the number of CuO_2 layers in the unit cell.[16] This means that the energy of the kink is independent of T_c, which is also an argument in favor of a phononic coupling as well as the fact that the kink in dispersion in the nodal direction persists even above $T^{\star}$.

The scenario of a coupling to a resonant magnetic mode as claimed previously by some authors based on photoemission data evaluation[2,3,5] is therefore not supported by our

results. But besides ours, also a number of other observations are in favor of the phononic-mode-coupling scenario. Lanzara *et al.*[18] found that the kink energy is ubiquitous: it occurs independently of the gap energy on the same energy scale for differently and even overdoped samples of various high-T_c families and even in LSCO. LSCO is known to possess no clear magnetic mode at all. The magnetic-mode energy for the other high-T_c cuprates scales with doping.[19] Recently even several bosonic modes have been identified in the electron self energy of underdoped LSCO by high-resolution ARPES.[20] The multiple features show marked differences from the magnetic excitation spectra measured in LSCO which are mostly featureless. They resemble more the phonon density of states from neutron measurements.

V. SUMMARY

Along the nodal direction all samples, especially the optimally doped samples, showed a kink in the dispersion of the main band. Around the position of the kink in the dispersion curve at $\hbar\omega_{\mathrm{kink}}=(64\pm6)$ meV appeared a drop in the FWHM curve. This means that above $\hbar\omega_{\mathrm{kink}}$ the electronic system couples very effectively to a collective mode and is therefore strongly damped. Additionally, we found a kink in the peak height. This kink in the peak height appeared at the same position as the kink in the dispersion and the drop in the width and allows a more precise determination of the kink position. It can be explained as an indicator of a shift of the spectral weight to lower binding energies.

The shadow band behaved analogously concerning the kink in the dispersion curve and the drop in the FHWM curve. Because the intensity of the shadow band is much lower than the intensity of the main band, it was not possible to determine a kink in the peak height also for the shadow band.

In agreement with former published literature the kink in dispersion appears independently of temperature and only sharpens at lower temperature. The drop in the FWHM curves persists at temperatures higher than T_c, but disappears near $T^{\star}$. The latter is also valid for the kink in peak height, which shows that the observed kink in the peak height is closely connected with the kink in the dispersion and the drop in the width.

Possible reasons for the kink in the peak height, the kink in the dispersion, and the drop in the width are coupling to a magnetic or to a phononic mode. The main difference between these two scenarios is the scaling of the magnetic-mode energy with T_c. But such a scaling of the energy of the kink could not be observed here and is also not in the published literature. Therefore it is very likely that phononic coupling is responsible at least for the kink in the nodal direction.

ACKNOWLEDGMENTS

We gratefully thank the staff of the Synchrotron Radiation Center in Madison-Wisconsin for the excellent support during the measurements and the DFG for financial support. This work is based upon research conducted at the Synchrotron Radiation Center, University of Wisconsin-Madison, which is supported by the NSF under Grant No. DMR-0084402.

[1] T. Valla, A. V. Fedorov, P. D. Johnson, B. O. Wells, S. L. Hulbert, Q. Li, G. D. Gu, and N. Koshizuka, Science **285**, 2110 (1999).
[2] A. Kaminski, M. Randeria, J. C. Campuzano, M. R. Norman, H. Fretwell, J. Mesot, T. Sato, T. Takahashi, and K. Kadowaki, Phys. Rev. Lett. **86**, 1070 (2001).
[3] A. A. Kordyuk, S. V. Borisenko, A. Koitzsch, J. Fink, M. Knupfer, B. Büchner, H. Berger, G. Margaritondo, C. T. Lin, B. Keimer, S. Ono, and Y. Ando, Phys. Rev. Lett. **92**, 257006 (2004).
[4] A. A. Kordyuk, S. V. Borisenko, V. B. Zabolotnyy, J. Geck, M. Knupfer, J. Fink, B. Büchner, C. T. Lin, B. Keimer, H. Berger, and A. V. Pan, Seiki Komiya, and Y. Ando, Phys. Rev. Lett. **97**, 017002 (2006).
[5] A. Koitzsch, S. V. Borisenko, A. A. Kordyuk, T. K. Kim, M. Knupfer, J. Fink, M. S. Golden, W. Koops, H. Berger, B. Keimer, C. T. Lin, S. Ono, Y. Ando, and R. Follath, Phys. Rev. B **69**, 220505(R) (2004).
[6] A. Mans, I. Santoso, Y. Huang, W. K. Siu, S. Tavaddod, V. Arpiainen, M. Lindroos, H. Berger, V. N. Strocov, M. Shi, L. Patthey, and M. S. Golden, Phys. Rev. Lett. **96**, 107007 (2006).
[7] M. Eschrig and M. R. Norman, Phys. Rev. B **67**, 144503 (2003).
[8] P. V. Bogdanov, A. Lanzara, S. A. Kellar, X. J. Zhou, E. D. Lu, W. J. Zheng, G. Gu, J.-I. Shimoyama, K. Kishio, H. Ikeda, R. Yoshizaki, Z. Hussain, and Z. X. Shen, Phys. Rev. Lett. **85**, 2581 (2000).
[9] P. D. Johnson, T. Valla, A. V. Fedorov, Z. Yusof, B. O. Wells, Q. Li, A. R. Moodenbaugh, G. D. Gu, N. Koshizuka, C. Kendziora, Sha Jian, and D. G. Hinks, Phys. Rev. Lett. **87**, 177007 (2001).
[10] A. Koitzsch, S. V. Borisenko, A. A. Kordyuk, T. K. Kim, M. Knupfer, J. Fink, H. Berger, and R. Follath, Phys. Rev. B **69**, 140507(R) (2004).
[11] H. F. Fong, P. Bourges, Y. Sidis, L. P. Regnault, A. Ivanov, G. D. Gu, N. Koshizuka, and B. Keimer, Nature (London) **398**, 588 (1999).
[12] H. He, Y. Sidis, P. Bourges, G. D. Gu, A. Ivanov, N. Koshizuka, B. Liang, C. T. Lin, L. P. Regnault, E. Schoenherr, and B. Keimer, Phys. Rev. Lett. **86**, 1610 (2001).
[13] Pengcheng Dai, H. A. Mook, S. M. Hayden, G. Aeppli, T. G. Perring, R. D. Hunt, and F. Doğan, Science **284**, 1344 (1999).
[14] I. Eremin, D. K. Morr, A. V. Chubukov, K. H. Bennemann, and M. R. Norman, Phys. Rev. Lett. **94**, 147001 (2005) and references therein.
[15] Y. Petrov, T. Egami, R. J. McQueeney, M. Yethiraj, H. A. Mook, and F. Dogan, arXiv:cond-mat/0003414 (unpublished).
[16] T. Sato, H. Matsui, T. Takahashi, H. Ding, H.-B. Yang, S.-C. Wang, T. Fujii, T. Watanabe, A. Matsuda, T. Terashima, and K. Kadowaki, Phys. Rev. Lett. **91**, 157003 (2003).
[17] X. J. Zhou, T. Yoshida, A. Lanzara, P. V. Bogdanov, S. A. Kellar,

K. M. Shen, W. L. Yang, F. Ronning, T. Sasagawa, T. Kakeshita, T. Noda, H. Eisaki, S. Uchida, C. T. Lin, F. Zhou, J. W. Xiong, W. X. Ti, Z. X. Zhao, A. Fujimori, Z. Hussain, and Z.-X. Shen, Nature (London) **423**, 398 (2003).

[18] A. Lanzara, P. V. Bogdanov, X. J. Zhou, S. A. Kellar, D. L. Feng, E. D. Lu, T. Yoshida, H. Eisaki, A. Fujimori, K. Kishio, J.-I. Shimoyama, T. Noda, S. Uchida, Z. Uchida, Z. Hussain, and Z.-X. Shen, Nature (London) **412**, 510 (2001).

[19] Y. Sidis, S. Pailhes, B. Keimer, P. Bourges, C. Ulrich, and L. P. Regnault, Phys. Status Solidi B **241**, 1204 (2004).

[20] X. J. Zhou, Junren Shi, T. Yoshida, T. Cuk, W. L. Yang, V. Brouet, J. Nakamura, N. Mannella, Seiki Komiya, Yoichi Ando, F. Zhou, W. X. Ti, J. W. Xiong, Z. X. Zhao, T. Sasagawa, T. Kakeshita, H. Eisaki, S. Uchida, A. Fujimori, Zhenyu Zhang, E. W. Plummer, R. B. Laughlin, Z. Hussain, and Z.-X. Shen, Phys. Rev. Lett. **95**, 117001 (2005).